sciendo

ANNALS OF WEST UNIVERSITY OF TIMISOARA PHYSICS
Vol. LXV, 2023

DOI: 10.2478/awutp-2023-0012

STRUCTURAL AND THERMODYNAMIC PROPERTIES OF Cu_2ZnSnS_4 MATERIAL: THEORETICAL PREDICTION

L. Boutahar [1], A. Benamrani [2], Z. Rouabah [1], S. Daoud [1,*]

[1]*Laboratoire Matériaux et Systèmes Electroniques, Université Mohamed Elbachir El Ibrahimi de Bordj Bou Arreridj, Bordj Bou Arreridj, 34000, Algérie*
[2]*Laboratory of Materials Physics, Radiation and Nanostructure (LPMRN), University Mohamed El Bachir El Ibrahimi of Bordj Bou Arreridj, 34000 Bordj Bou-Arreridj, Algeria*
**Corresponding author E-mail:salah_daoud07@yahoo.fr*

Article Info

Received: 02.09.2023
Accepted: 02.11.2023

Keywords:

Cu_2ZnSnS_4 material, Thermodynamic properties, DFT, Quantum Espresso

Abstract

The present work aims to investigate the structural and thermodynamic properties of homogenous tetragonal Cu_2ZnSnS_4 (CZTS) absorber material in Kesterite phase using first-principle calculations based on density functional theory (DFT). This approach requires only knowledge of the atomic species and crystal structure to predict several physical properties of materials. The Quantum Espresso code within the Ultra Soft pseudopotentials (USPP) and the local density approximation (LDA) were used in the calculations. Equilibrium unit cell volumes, bulk modulus, as well as the pressure derivative of the bulk modulus are predicted. In addition, several thermodynamic properties, especially: the Debye's vibrational energy, the vibrational free energy, the vibrational entropy, and the constant volume heat capacity at different temperatures T of Cu_2ZnSnS_4 material are calculated and discussed. Our study shows that the vibrational energy, the entropy and the constant volume heat capacity increase with increasing temperature, while the vibrational free energy decreases monotonously with the increase of temperature.

1. Introduction

Interest in developing clean and sustainable electricity sources continues to grow, with high levels of investment in renewable energy technologies. Photovoltaic (PV) panels are one promising and fast-growing industry in these technologies [1]. Cu_2ZnSnS_4 (CZTS) quaternary semiconducting compound has emerged as one of the promising absorber layer materials for thin film solar cell application [2], this because the CZTS material exhibits a near-optimum direct band gap of ~ 1.5 eV and it has a large absorption coefficient, which is in order of 10^4 cm^{-1} [3]. Cu_2ZnSnS_4 compound is also one a potential Cu-based thermoelectric (TE) material

[4]. Because of their low price and non toxicity, recently Cu-based materials have been proposed as a new class of thermoelectric materials [4].

Yu and Carter [1] investigated theoretically the stabilities of three phases (kesterite, stannite, and wurtzite) of the CZTS material using density functional theory (DFT) method, while Zhang *et al.* [5] studied the geometric, electronic and photo-electro-catalytic properties of a Cu_2ZnSnS_4 monolayer (CZTS ML) using the same method. Using X-ray diffraction (XRD), UV-VIS spectroscopy, Raman spectroscopy (RS), and scanning electron microscope (SEM) techniques, Parthibaraj *et al.*[2] studied the morphology and the optical properties of polycrystalline Cu_2ZnSnS_4 thin film, while Lydia and Sreedhara Reddy [6] investigated experimentally the structural parameters and the optical properties of Cu_2ZnSnS_4 nanoparticles. By sulfurization of Cu/ZnSn/Cu precursor in sulfur atmosphere, Chalapathy and co-authors [7] elaborated Cu_2ZnSnS_4 thin films with a conversion efficiency of around 4.6%.

In the present work, we report on first-principles calculations of the structural parameters and thermodynamic properties of CZTS material using the Quantum Espresso (QE) code [8, 9] and the package Thermo_pw [10]. Several thermodynamic properties, especially the Debye's vibrational energy U_{ph}, the vibrational free energy F_{vib}, the vibrational entropy S, and the constant volume heat capacity C_V in the temperature ranging from 0 to 800 K of Cu_2ZnSnS_4 material are reported and analyzed. In order to simplify our study, we limited our calculations only at zero-pressure.

2. Computational method

In this work, we employed the Quantum Espresso code with thermo_pw tool [8-10], which is based on the pseudopotential (PP) method and a plane-wave basis set. We used the Ultra Soft pseudopotentials (USPP) form [11], while the exchange correlation potential was examined using the local density approximation (LDA). For the LDA approach, we used the Perdew-Zunger (PZ) exchange correlation functional [12].

In the present work, the wave functions were expanded with an energy cut-off = 80 Ry for the plane-wave basis set, while the charge density cut-off was taken 800 Ry, conducting a convergence with an energy threshold of $1x10^{-4}$ Ry. The integration over the Brillouin zone was performed using 4x4x2 k-points Monkhorst-Pack mesh [13].

3. Results and discussion

3. 1. Structural parameters

The crystallographic structures of CZTS belong to conventional body-centered tetragonal

unit cells with $I\bar{4}$ space group (No. 82) for the Kesterite phase [14, 15]. In this structure, the molecule consists of 8 atoms (8 atoms in their primitive unit cell), while the conventional unit cell contains 16 atoms. The two inequivalent Cu atoms occupy the Wyckoff positions at *2a* and *2c*, while Zn and Sn atoms are located at *2d* and *2b* sites, respectively. This results in alternating cation layers of CuSn, CuZn, CuSn, and CuZn at z = 0, 1/4, 1/2, and 3/4, respectively, while the S atoms are located at *8g* (x, y, z) position [14] (For more details please see for example the Refs. [14, 15]).

The calculated total energies *E* for the Kesterite phase are plotted in Fig.1, as a function of the volume *V* of unit cell. From the *E*-*V* data plotted in Fig.1, it is possible to obtain the static structural properties from the volume which gives the minimum energy, the bulk modulus B_0 and the pressure derivative of the bulk modulus B_0'. The procedure consisted of fitting the values of total energy as a function of the unit cell volume using the Murnaghan equation of state [16].

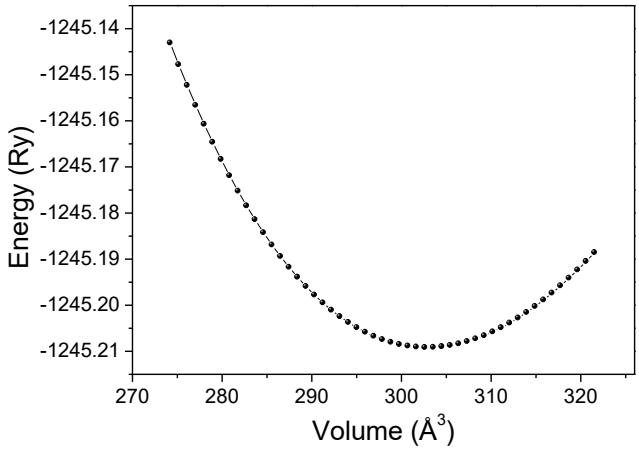


Figure 1. E-V data of CZTS material in Kesterite phase

The numerical values of the equilibrium volume V_0, bulk modulus B_0 and the pressure derivative of the bulk modulus B_0' were found to be 302.9 Å^3, 87.5 GPa and 4.70, respectively. Our results of the optimized lattice parameters a, c and the bulk modulus B_0 are also summarized in the Table 1, along with the experimental [15, 17, 18] and theoretical [1] data obtained by other authors. Our results of the lattice parameters $a$and$c$ are slightly lower than the experimental ones (a = 5.4232 Å, and c = 10.8225 Å) measured at 4 K for the Sn-poor and Cu-rich sample [15]. The value (87.5 GPa) of B_0 of CZTS obtained in this study is equal exactly to the theoretical value (87.5 GPa) obtained from the elastic constants C_{ij} reported by Boutahar *et al.* [19].

Table. 1 The optimized lattice parameters and bulk modulus, compared with experimental [15, 17, 18] and other theoretical [1] data. [a][15], [b][17], [c][18], [d][1] . Using empirical formula*

Material		Method	a(Å)	c(Å)	$B_0(GPa)$
	Present	LDA(PZ)	5.327	10.665	87.5
Cu_2ZnSnS_4	Exp.		5.4232[a]	10.8225[a]	83.6*[c]
			5.455[b]	10.880[b]	-
	Others.	PBE	5.475[d]	10.938[d]	69.7[d]
		PBE+U	5.444[d]	10.866[d]	66.5[d]

Knowledge of the variation in pressure with volume for a single phase determines the equilibrium volume V_0, and gives also access to the bulk modulus B and its pressure derivative B_0' [20]. The procedure consisted of fitting the values of pressure as functions of the normalized volume (V/V_0) using the third-order Vinet equation of state (EoS) equation of state [21].

Figure 2 gives a plot of the normalized volume (V/V_0) as a function of pressure of Cu_2ZnSnS_4 material at zero-temperature. We observed that V/V_0 of CZTS has almost linearly decreased with the increase of pressure as shown in Fig. 2. The numerical values of V_0, B_0 and B_0' were found to be 302.9 Å^3, 87.2 GPa and 4.96, respectively. All these results are in very good agreement with the values obtained from the E-V data. The deviation between our obtained value (87.2GPa) of B_0 and the theoretical result (88.37GPa) reported by Gunaicha *et al.*[22] is only around 1.33%.

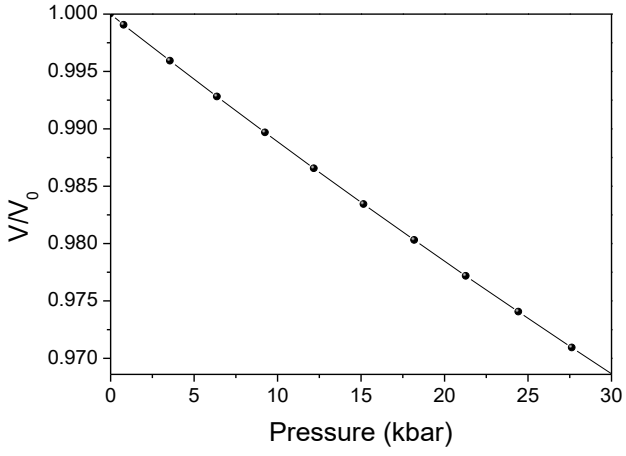


Figure 2. Variations of V/V_0 of Cu_2ZnSnS_4 as a function of pressure up to 30 kbar

3. 2. Bulk modulus and bulk sound wave velocity

If a large hydrostatic pressure was applied, the concept of the nonlinear terms in elastic properties investigation was usually used, but for many technological applications, it is

sufficient to consider only the linear terms. If we consider only the linear term of the bulk modulus, this later can be given as a function of pressure as follows: $B(p) = B_0 + B_0' p$ [23], where B_0 and B_0' are the equilibrium bulk modulus and its pressure derivative, respectively. So, the pressure dependence of B of CZTS is given by the following expression: $B(p) = 87.2 + 4.96\,p$. The variations of $B(p)$ of CZTS as a function of pressure up to 30 kbar are plotted in Fig. 3.

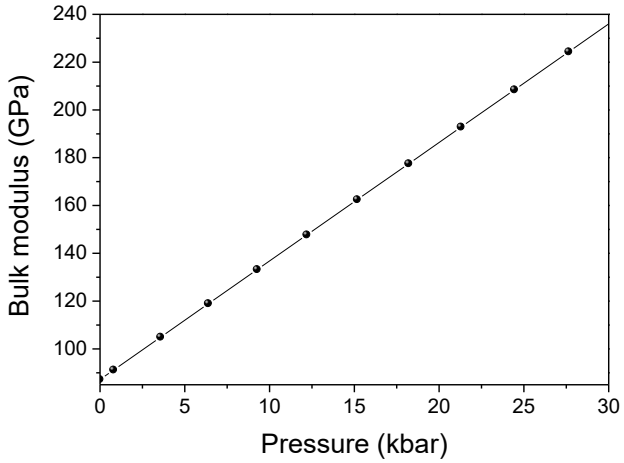


Figure 3. Variations of the bulk modulus B of Cu_2ZnSnS_4 as a function of pressure up to 30 kbar

Bulk sound wave velocity v_B was usually calculated by $v_B = (B/\rho)^{1/2}$[19], where ρ is the crystal density, and B is the bulk modulus. The obtained values of the bulk sound wave velocity of Cu_2ZnSnS_4 material were illustrated in Fig. 4. Since the sound wave velocity v_B obtained from the previous equation has polynomial curve as function of the pressure, we fit the data with second order polynomial to determine v_B (expressed in km/s) as function of pressure p (given in kbar) that can be expressed as: $v_B = 4.2658 + 0.11\,p - 7.62 \times 10^{-4}\,p^2$.

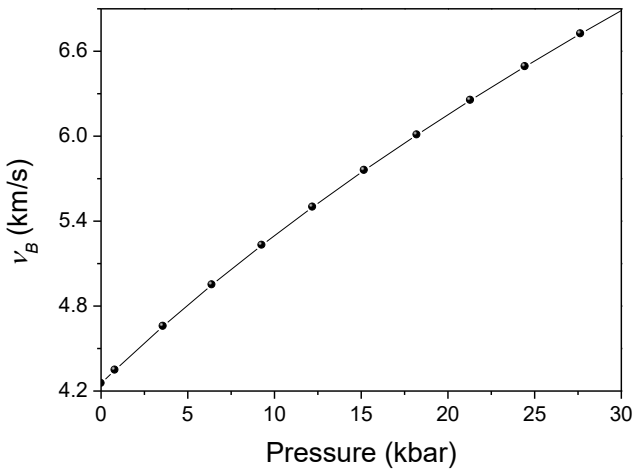


Figure 4. Bulk sound velocity v_B versus pressure up to 30 kbar for CZTS material

3. 3. Debye's vibrational energy

Within the quasi-harmonic approximation, the internal energy of a solid is the sum of three terms: the ground state energy U_0 (obtained with DFT), the electronic energy U_{el} due to finite temperature of electrons and the vibrational energy U_{ph} due to phonon contribution to the internal energy of the solid. The internal energy U at a given temperature T and volume V is defined as:

$$U = U_0 + U_{el} + U_{ph} \tag{1}$$

The Debye's vibrational energy per cell is defined as [24]:

$$U_{ph} = \frac{1}{N}\left(\sum_{\boldsymbol{q},\eta} \frac{\hbar\omega_{\boldsymbol{q},\eta}}{2} + \sum_{\boldsymbol{q},\eta} \frac{\hbar\omega_{\boldsymbol{q},\eta}}{e^{\hbar\omega_{\boldsymbol{q},\eta}/K_B T} - 1}\right) \tag{2}$$

where N is the number of cells in our crystal of interest, $\hbar$ is the reduced Planck constant, K_B is the Boltzmann constant, q is the wave-vector and η is phonon mode.

It is well known that if the E-V data of any system is known, usually several other thermophysical quantities which are related to the total energy E can be obtained computationally [25-27]. Fig.5 illustrates the Debye's vibrational energy U_{ph} as a function of temperature for Cu_2ZnSnS_4 material at zero-pressure. At zero-temperature the Debye's vibrational energy U_{ph} was found to be 49.31 kJ $N^{-1}mol^{-1}$, while at 298 K it is found to be at around 126.24 kJ $N^{-1}mol^{-1}$.

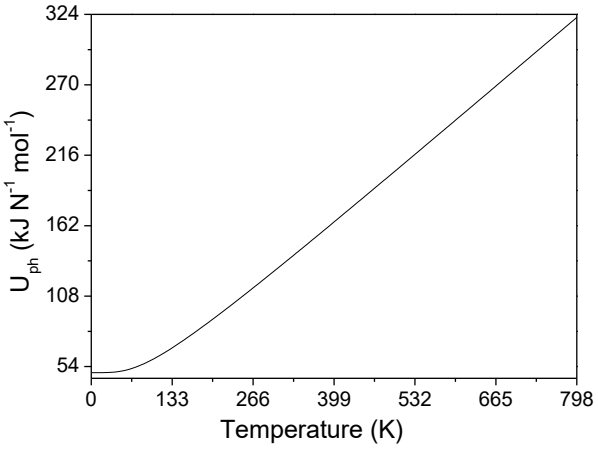


Figure 5. Variations vibrational energy U_{ph} of CZTS material as a function of temperature T

3. 4. Vibrational free energy

We further explore the vibrational free energy F_{vib} of our material of interest. F_{vib} is given by the following expression [28]:

$$F_{vib}(\varepsilon,T)=\frac{1}{2N}\sum_{q,\eta}\hbar\omega_{\eta}(q,\eta)+\frac{K_BT}{N}\sum_{q,\eta}\ln\left[1-\exp\left(-\frac{\hbar\omega_{\eta}(q,\eta)}{K_BT}\right)\right] \quad (3)$$

In Eq. (3), the summation is taken over phonon frequencies $\omega_{\eta}(q,\eta)$, where q denotes the wave vectors with the first Brillouin zone and η the different phonon branches.

In Fig.6, we have plotted the F_{vib} as a function of the temperature T for CZTS in the Kesterite phase at zero-pressure. We observed that the vibrational free energy F_{vib} decreases non-linearly with increase of T. At zero-temperature the F_{vib} was found to be 49.3 kJ.N^{-1}.mol^{-1}, while at 298 K it is found to be at around -24.2 Kj.N^{-1}.mol^{-1}. It can be noted that at zero-temperature both the vibrational energy U_{ph} and the free energy F_{vib} have same values for our material of interest.

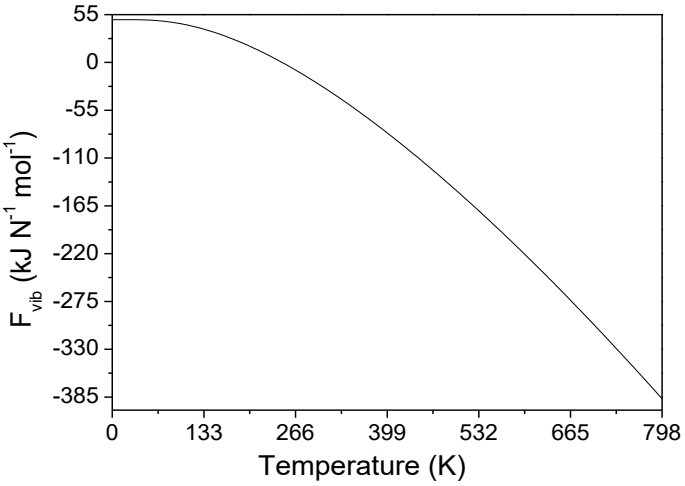


Figure 6. Variations of the vibrational free energy F_{vib} of CZTS as a function of temperature T

Our data regarding the vibrational free energy F_{vib} versus temperature for CZTS material at zero-pressure are fitted by a least-squares procedure. The correlation between F_{vib} (expressed in kJN^{-1}mol^{-1}) and T (expressed in K) is given by the following expression: F_{vib}= 50.42 + 0.036T- 0.11 × $10^{-2}T^2$ + 0.45 × $10^{-6}T^3$. It can be seen that similar qualitative behaviors have been reported for F_{vib} versus temperature for cubic $LiAl_2M$ (M = Rh, Pd, Ir and Pt) compounds [29] and cubic rock-salt scandium mono-phosphide (ScP) semiconducting material [30].

3. 5. Vibrational entropy

Using Thermo_pw package at a certain temperature T and having the internal energy U and the Helmholtz free energy F, the entropy can be calculated according to the equation: S =

$(U - F)/T$. The variations of the vibrational entropy S of CZTS material as a function of temperature in the range of 0 K to 800 K was shown in Fig.7.

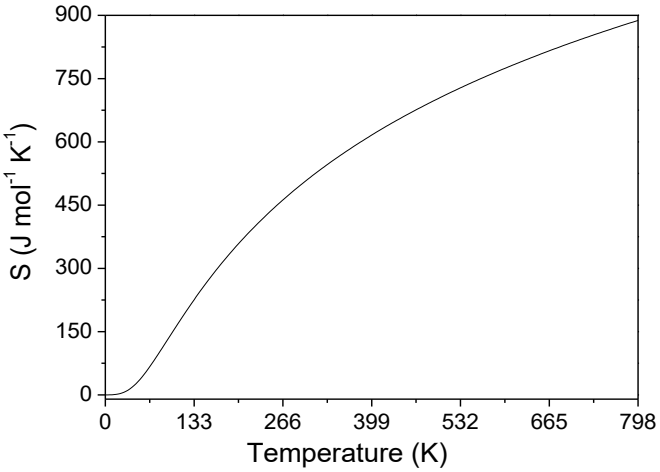


Figure 7. Entropy S of Cu_2ZnSnS_4 material versus temperature T

As the temperature increases, the vibrational entropy S of CZTS increase monotonously with the temperature T. At low temperatures, one can observe that the vibrational entropy S increases quickly with rising the temperature. At 298 K, the vibrational entropy S is found to be 504.76 $J.mol^{-1}.K^{-1}$.It can be noted that similar qualitative behaviors have been reported for S versus T for cubic rock-salt scandium mono-phosphide (ScP) [30], boron arsenide (BAs) semiconductor [31] and cubic CsCl-type Yttrium-Rhodium (YRh) intermetallic compound [32].

3. 6. Constant volume heat capacity

Heat capacity reflects the heat storage capacity or heat release capacity of solid materials [33]. Knowledge of the heat capacity of a substance provides essential insight into its vibrational properties, it is also mandatory for many applications [20]. Within the harmonic approximation, the isochoric heat capacity is given by the following equation [28]:

$$C_V = \frac{K_B}{N}\sum_{\boldsymbol{q}\upsilon}\left(\frac{\hbar\omega_\eta(\boldsymbol{q})}{K_BT}\right)^2 \frac{e^{\hbar\omega_\eta(\boldsymbol{q})/K_BT}}{(e^{\hbar\omega_\eta(\boldsymbol{q})/K_BT}-1)^2} \quad (4)$$

In Fig.8, we have plotted the constant volume heat capacity C_V as a function of the temperature T for CZTS material in the Kesterite phase at zero-pressure. It can be seen from Fig.8 that the C_V of Cu_2ZnSnS_4 material increases exponentially with the temperature for T <

400 K, while for high temperature, it approaches the DuLong-Petit limit, indicating that at high temperature, all phonon modes are sufficiently excited by the thermal energy [34].

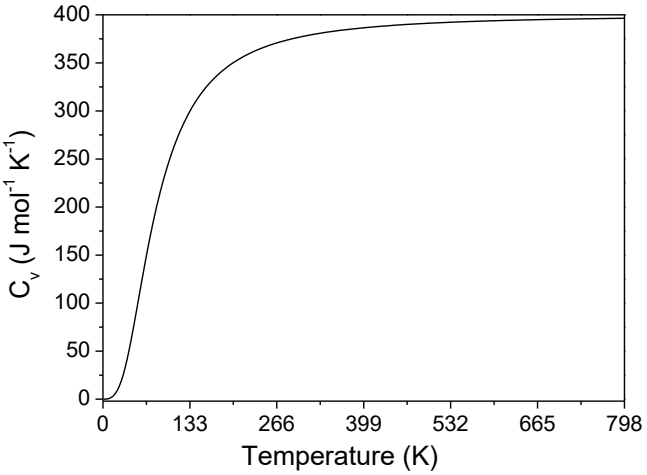


Figure 8. Constant volume heat capacity C_V of Cu_2ZnSnS_4 versus temperature T

Due to general laws of thermodynamics and the same nature of materials as semiconductors, it can be observed that similar qualitative behaviors from the quantitative point of view have been reported for C_V versus temperature for ScP material [32], copper chloride (CuCl) and copper bromide (CuBr) compounds [34], group Ⅲ-phosphide semiconducting materials [35], for boron antimonide (BSb) compound in cubic zinc-blende structure [36], and for both $Cd_{0.75}Cr_{0.25}Se$ and $Zn_{0.75}Cr_{0.25}S$ ternary materials [37]. At 298 K, the constant volume heat capacity C_V was found to be at around 376.44 Jmol^{-1}K^{-1}.

4. Conclusions

The ground state parameters as well as the thermodynamic properties of CZTS material in the Kesterite phase have been calculated and analyzed using the Ultra Soft pseudopotentials in the framework of the DFT as implemented in the Quantum Espresso code. All our results of the ground state parameters obtained from both *E-V* data and *P-V* data agree well with other data of the literature. Our study shows that the vibrational energy and the vibrational entropy increase monotonously with increasing temperature *T*, while the vibrational free energy decreases with rising the temperature. The constant volume heat capacity C_V increases exponentially with the temperature for T < 400 K, while for high temperature all phonon modes are sufficiently excited by the thermal energy, rending C_V approaches to the Dulong-Petit limit.

References

[1] K. Yu, E. A. Carter, *Chem. Mater*., 27 (2015) 2920

[2] V. Parthibaraj, K. Tamilarasan, K. S. Pugazhvadivu, C. Rangasami, IJIRSET.4 (2015) 670

[3] H. Katagiri, K. Saitoh, T. Washio, H. Shinohara, T. Kurumadani, S. Miyajima, *Sol. Energy Mater. Sol. Cells*.,65 (2001) 141

[4] B. Wang, H. Xiang, T. Nakayama, J. Zhou, B. Li, *Phys. Rev. B*,95 (2017) 035201

[5] R. Zhang, X. Wen, F. Xu, Q. Zhang, L. Sun, *J. Phys. Chem.* C, 124, (2020) 11922

[6] R. Lydia, P. Sreedhara Reddy, J. *Nano- Electron. Phys*.,5No 3, (2013) 03017

[7] R.B.V. Chalapathy, G. S. Jung, B. T. Ahn, Sol. Energy Mater. Sol. Cells, 95 (2011) 3216

[8] S. Baroni, A. DalCorso, S. deGironcoli, P. Giannozzi, *Rev. Med. Phys*., 73 (2001) 515

[9] S. Scandolo, P. Giannozzi, C. Cavazzoni, S. deGironcoli, A. Pasquarello, S. Baroni, *Z. Kristallogr.* 220, (2005) 574

[10] A. Dal Corso, *J. Phy. Condens. Matter*., 28 (2016) 075401

[11] D. Vanderbilt, *Phys. Rev. B*, 41 (1990) 7892

[12] J.P. Perdew, A. Zunger, *Phys. Rev. B*, 23 (1981) 5048

[13] H.J. Monkhorst, J.D. Pack, *Phys. Rev. B,* 13 (1976) 5188

[14] M. Dimitrievska, F. Boero, A. P. Litvinchuk, S. Delsante, G. Borzone, A. Perez-Rodriguez, V. Izquierdo-Roca, *Inorg. Chem*., 56 (2017) 3467

[15] C.J. Bosson, M.T. Birch, D.P. Halliday, K.S. Knight, A.S. Gibbs, P.D. Hatton, *J. Mater. Chem. A.*, 5 (2017) 16672

[16] F. D, Murnaghan, *Proc. Natl. Acad. Sci.* USA, 30 (1944) 244

[17] A. Nagaoka, K. Yoshino, H. Taniguchi, T. Taniyama, H. Miyake, *J. Cryst. Growth*, 341 (2012) 38

[18] A. Nagaoka, K. Yoshino, K. Aoyagi, T. Minemoto, Y. Nose, T. Taniyama, K. Kakimoto, H. Miyake, *J. Cryst. Growth,* 393 (2014) 167

[19] L. Boutahar, A. Benamrani, Z. Er, N. Bioud, Z. Rouabah, *Annals of West University of Timisoara Physics,* 64 (2022) 55

[20] N. Bioud, K. Kassali, X-W. Sun, T. Song, R. Khenata, S. Bin-Omran, *Mater. Chem. Phys*., 203 (2018) 362

[21] P. Vinet, J. R. Smith, J. Ferrante, J.H. Rose, *Phys. Rev. B*, 35 (1987) 1945

[22] P. P. Gunaicha, S. Gangam, J. L. Roehl, S. V. Khare, *Sol. Energy,* 102 (2014) 276

[23] S. B. Zhang, M. L. Cohen, *Phys. Rev. B*, 35 (1987) 7604

[24] K. Yaddanapudi, *Comp. Mater. Sci*., 184 (2020) 109887

[25] N. Bioud, X-W. Sun, S. Daoud, T. Song, R. Khenata, S. Bin Omran, *Optik,* 155 (2018) 17

[26] S. Amari, S. Daoud, *Comput. Condens. Matter*, 33 (2022) e00764

[27] S. Daoud, N. Bouarissa, H. Rekab-Djabri, P. K. Saini, *Silicon,* 14 (2022) 6299

[28] C. Malica, A. Dal Corso, *J. Appl. Phys*., 127 (2020) 245103

[29] A. Benamrani, S. Daoud, N. Bouarissa, *Eur. Phys. J. B*.,95 (2022) 106

[30] A. Benamrani, S. Daoud, P.K. Saini, *J. Nano- Electron. Phys.*,13No 1 (2021) 01008

[31] S. Daoud, N. Bioud, N. Lebga, *Chinese J. Phys.,* 57 (2019) 165

[32] A. Benamrani, S. Daoud, Manal M. Abdus Salam, H. Rekab-Djabri, *Mater. Today Commun.*, 28 (2021) 102529

[33] S. G. Zhou, M. L. Tian, Y. Xu, C. Zhang, Y. Cao, *Indian J. Phys.,* 96 (2022) 3449

[34] N. Bioud, N. Bouarissa, K. Kassali, *J. Electron Mater.,* 46 (2017) 2521

[35] J. Wu, J. Li, Y. Yu, Y. Yu, *CIESC Journal,* 71 (2020) 192

[36] N. Bioud, X.-W. Sun, S. Daoud, T. Song, and Z.J. Liu, *Mater. Res. Express*, 5 (2018) 085904

[37] S. Amari, S. Daoud, H. Rekab-Djabri, *Acta Phys. Pol. A*, 143 (2023) 36